Nanostructure of Edge Dislocations in a Smectic-C^* Liquid Crystal

C. Zhang,[1] A. M. Grubb,[2] A. J. Seed,[2] P. Sampson,[2] A. Jákli,[1] and O. D. Lavrentovich[1,*]
[1]Liquid Crystal Institutes, Kent State University, Kent, Ohio 44242, USA
[2]Department of Chemistry and Biochemistry, Kent State University, Kent, Ohio 44242, USA
(Received 19 June 2015; published 20 August 2015)

We report on the first direct nanoscale imaging of elementary edge dislocations in a thermotropic smectic-C^* liquid crystal with the Burgers vector equal to one smectic layer spacing d. We find two different types of dislocation profiles. In the dislocation of type A, the layers deformations lack mirror symmetry with respect to the plane perpendicular to the Burgers vector; the dislocation core size is on the order of d. In the dislocation of type S, the core is strongly anisotropic, extending along the Burgers vector over distances much larger (by a factor of 4) than d. The difference is attributed to a different orientation of the molecular tilt plane with respect to the dislocation's axis; the asymmetric layers distortions are observed when the molecular tilt plane is perpendicular to the axis and the split S core is observed when the molecules are tilted along the line.

DOI: 10.1103/PhysRevLett.115.087801 PACS numbers: 61.30.Jf, 61.30.Cz, 61.72.Ff, 61.72.Lk

Linear defects in materials with broken translational symmetry, called dislocations, determine many static and dynamic properties of these materials [1]. The structure and behavior of dislocations is relatively well studied for the case of regular solids, especially metals [2]. Dislocations in soft matter, such as smectic liquid crystals and block copolymers, play a similarly important role [1,3], as evidenced by rheological effects [4–8]. In some cases, such as the vicinity of a smectic A (SmA)-to smectic C (SmC) phase transition, accompanied by a tilt of molecules, the presence of dislocations can be verified by optical microscopy [9]. One of the important questions that remains unanswered is the structure of the dislocation core, i.e., the region at the "center" of the defect where the deformations are too strong to sustain the usual type of order. The spatial extension of the core is of the order of a few characteristic periods of the positional order, often being around (1–10) nm, which calls for imaging techniques such as electron microscopy, but the latter is limited by the soft nature of smectics and by the need to align the material. As a result, the nanometer-resolved images of dislocations are available only for very few smectic materials, such as the lamellar phospholipids [10] and bent-core thermotropic smectics [11].

In this work, using cryo-transmission electron microscopy (cryo-TEM), we present the first direct observation of edge dislocations in a thermotropic smectic-C^* (SmC^*) phase formed by rodlike chiral molecules. The study reveals two different types of elementary edge dislocations with the Burgers vector $b = d$, where d is the smectic periodicity. In the "asymmetric" type A, the layer deformations lack mirror symmetry with respect to the plane of the extra layer. In the "split" type S, the core is strongly anisotropic, extending along the Burgers vector $\mathbf{b}$ over the distances $2\xi_z$ much larger than the core size $2\xi_x$ measured in the direction perpendicular to $\mathbf{b}$. The observation of split S cores confirms a long-standing prediction by Allen and Kleman [12]. We suggest that the distinct A and S types are caused by the different direction of molecular tilt within the smectic layers, which is perpendicular to the dislocation's axis in the A case and parallel to it in the S case.

We used (*S*)-4-(1-methylheptyloxy) phenyl 4-(2-dodecyloxy-1,3-thiazol-5-yl) benzoate, abbreviated as AG14 [11]. In cooling, it exhibits the following phase sequence: Iso 104 °C SmA 102 °C SmC^* 72 °C Cr. In SmC^*, the normal $\hat{\boldsymbol{\nu}}$ to the layers is also the axis of the heliconical director $\hat{\mathbf{n}} = \{\sin\theta_0 \cos\varphi, \sin\theta_0 \sin\varphi, \cos\theta_0\}$; here θ_0 is the polar angle that the molecules make with $\hat{\boldsymbol{\nu}}$, $\varphi = \hat{q}z$ is the azimuthal direction of the molecular tilt, $\hat{q} = 2\pi/P$, and $P = 20$ μm is the heliconical pitch [11]. X-ray scattering shows a single peak at $q = 0.18$ Å^{-1} in the entire SmC^* range corresponding to the layer spacing $d_X = 34.9$ Å, which is smaller than the fully stretched molecular length of $l = 39$ Å, suggesting a tilt angle $\theta_X = 23.5$. The value is close to the optically measured $\theta_{\text{opt}} = 22 \pm 2$, determined by applying the electric field and finding the angular difference between two directions of the optical axis for opposite polarities of the field. When the material is sandwiched between two plasma-treated continuous carbon films, it shows a "bookshelf" chevron-free alignment of layers that are parallel to the probing electron beam; this alignment yields clear cryo-TEM images of the fine structure of edge dislocations.

Cryo-TEM measurements were carried out on a FEI Tecnai F20 microscope operating at 200 kV. A Gatan cryo-holder (model 626.DH) keeps the specimen temperature below −170 °C throughout the TEM observation. All images were recorded using a Gatan 4 K Ultra Scan CCD camera. The films were heated to the isotropic phase and cooled to the desired temperature, then quenched in

liquid nitrogen (−196 °C) to preserve the smectic structures [13].

The films were previewed at a dose of 20 e^-/nm^2; selected areas were then imaged at a dose of 200 e/nm^2, which we found did not cause any radiation damage. Previous studies of bent-core smectics carried out with this instrument visualized layers with a resolution ~0.7 nm [13–16]. The contrast in the cryo-TEM image, Fig. 1, is due to the difference in electron density of the aromatic core and the hydrocarbon tail. Lighter image areas in Fig. 1 correspond to hydrocarbon tails with lower electron absorption. To yield the contrast, the layers have to be parallel to the electron beam, with angular deviation less than $\alpha < \tan^{-1}(d/L)$. For $d \approx 4$ nm and for the film thickness $L \sim 100$ nm, this means $\alpha < 3$. The condition also implies that the periodicity d measured from the TEM images differs from the actual periodicity by less than 0.1%.

A typical TEM image of thin ($L \sim 100$ nm) samples quenched from the SmC^* phase at 98 °C shows a periodic intensity profile, indicating uniform alignment of smectic layers, Fig. 1(a). The fast Fourier transform (FFT) pattern, Fig. 1(b), obtained from a 300 nm × 350 nm area reveals $d = 3.83$ nm, which is close to $l = 3.9$ nm, but larger than the layer spacing 34.9 Å measured by X ray in the bulk. This indicates that the substrate reduces the director tilt to $\theta_o = \cos^{-1}(d/l) = \cos^{-1}(3.83/3.9) = 13°$ or even less; the same effect has been observed for other tilted smectics [14].

The elementary edge dislocations with Burgers vector $b = d$ are of two different types, A and S; see Figs. 2 and 3, respectively. To facilitate the discussion, we define two planes. One is the glide plane (GP) formed by the dislocation axis along the y axis, and its Burgers vector $\mathbf{b}$ along the z axis. In all experiments, GP is perpendicular to the plane xz of view. The second plane is the molecular tilt plane (MTP), determined by the local director $\hat{\mathbf{n}}$ and the smectic layers' normal $\hat{\boldsymbol{\nu}}$.

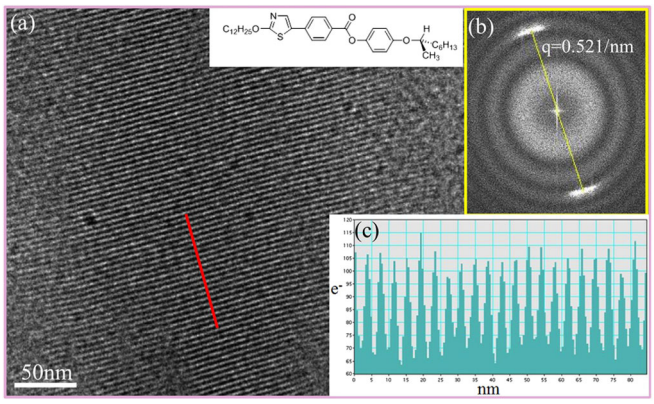

FIG 1 (color online). Typical cryo-TEM image of the studied material quenched from 98 °C. (a) 300 nm × 350 nm area showing uniform smectic layers normal to the substrate; inset shows the molecular structure. (b) The FFT image of the whole area showing the periodicity (2/0.521) nm = 38.3 Å. (c) The intensity profile along the red line marked in (a).

The A type edge dislocation is presented in Fig. 2(a), with one extra smectic layer (dark band labeled with "0") on the right-hand side. The core extends along the x and z axes by the similar distances $2\xi_x \approx 2\xi_z \approx d$, Fig. 2(c). The most notable feature is asymmetry of the layers displacements above [layers labeled with "+" in Fig. 2(c)] and below ("−" labels) the plane $z = 0$, i.e., $u(x, z) \neq -u(x, -z)$. In particular, the tilt of layers $\partial u/\partial x$ with respect to the x axis, is larger for $z < 0$ than for $z > 0$, Fig. 2(c). This is in sharp contrast to the symmetric edge dislocations observed in cholesterics [17] and bent-core smectics A [14] and with the theoretical predictions for smectics A [18–20].

The A dislocation in Fig. 2(a) is surrounded by layers in which the molecules tilt in the direction perpendicular to the dislocation. The FFT pattern in Fig. 2(b), corresponding to the real space image in Fig. 2(a), exhibits two sets of reflexes. The first set contains vertically spaced peaks associated with the layer periodicity $d = 3.83$ nm along the z axis. The second set is represented by two peaks located at the line that makes an angle about 10° with the z axis. The angle 10° agrees well with the estimate of the molecular tilt within the layers. The q value of the tilted peak infers a periodicity of 0.55 nm, which corresponds well to the distance between the thiazole and benzene ring [see inset in Fig. 1(a)] along the molecule. Therefore, the MTP is perpendicular to the GP in Fig. 2(a).

A very different S type of dislocation core is presented in Fig. 3. In this case, there are no clear FFT reflexes that could be associated with the molecular tilt in the xz plane of observation, suggesting that the molecules are tilted along the axis of dislocation. The S core is highly anisotropic, extending along the Burgers vector $\mathbf{b}$ over a distance $2\xi_z \approx 4d$ that is much larger that the core extension $2\xi_x \approx d$ measured in the direction perpendicular to the GP, Fig. 3(a). The anisotropic core involves multiple layers, $n > 1$, that are being disrupted and "melted" into a nematic-like region. In Fig. 3, there are $n = 4$ layers on one side of the GP and 5 layers on the other side that are disconnected. Figure 3(c) shows that the material density within the core (along the cut BB′) is practically constant over a large distance $2\xi_z \approx 4d$; the latter implies melting of the smectic positional order. Note that the average transmitted intensity is the same inside and outside the core, indicating that the average density of packing is practically the same.

The experiment demonstrates that the nanoscale structure of an edge dislocation depends on the angle φ between MTP and GP, which is close to either $\pi/2$ (type A dislocation) or 0 (S dislocation), Fig. 4. Cryo-TEM textures do not allow us to measure φ accurately; the conclusions that $\varphi = \pi/2$ in Fig. 2(a) and $\varphi = 0$ in Fig. 3(a) are based on whether the additional reflexes in FFT images are observed or not. In an ideal unbounded SmC^*, the angle $\varphi = \hat{q}z$ continuously changes along the z axis. However, since the pitch is very large, $P = 20$ μm, the TEM textures in Figs. 2(a) and 3(a) correspond to a practically constant φ;

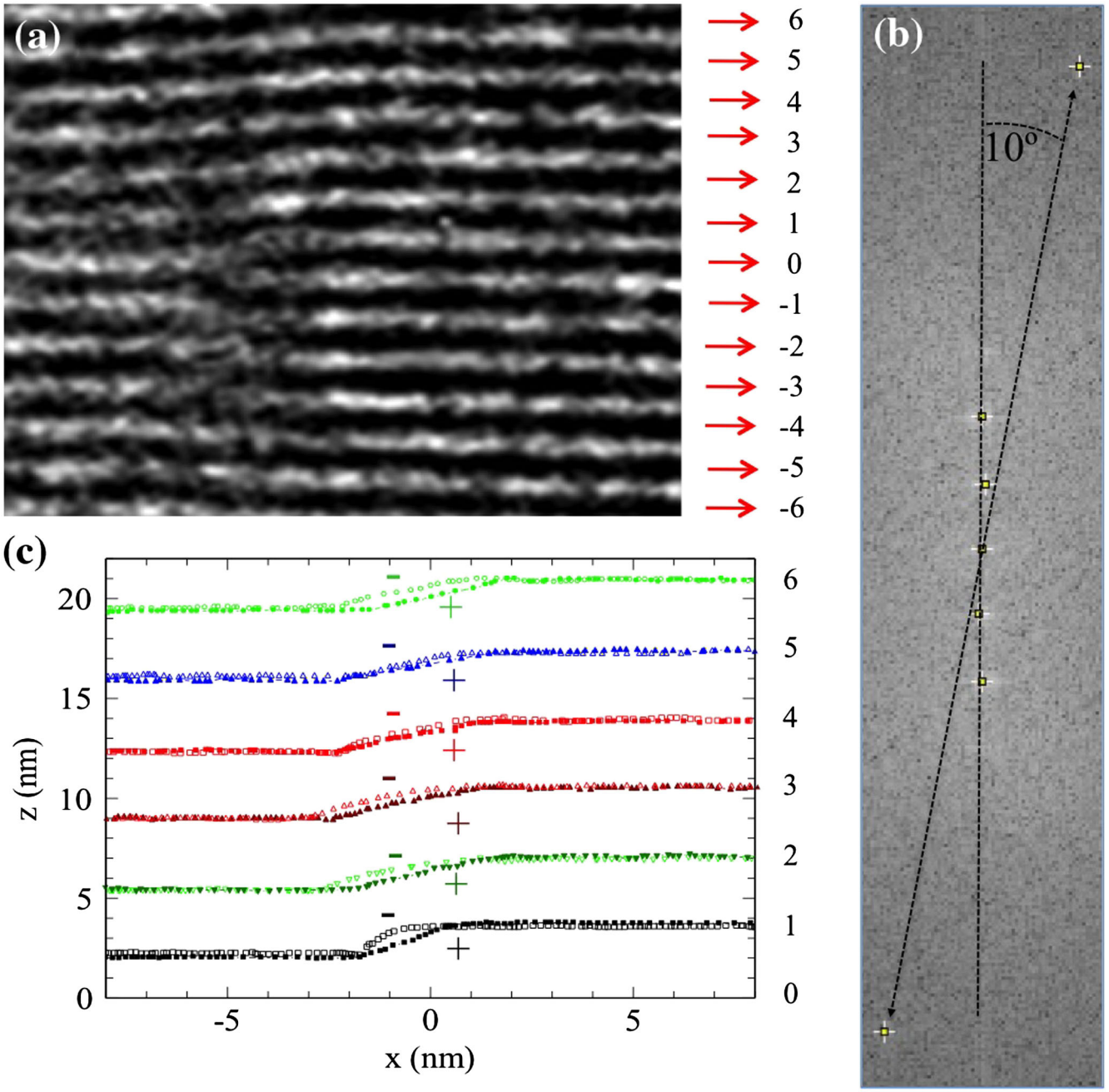

FIG. 2 (color online). Asymmetric-core A edge dislocation with the Burgers vector $b = d$. (a) TEM image; (b) FFT of the image in (a) showing the layered structure with $d = 3.83$ nm periodicity (peaks along the vertical line) and peaks along the line tilted by 10° from the vertical, corresponding to 0.55 nm periodicity. (c) The $x - z$ dependence of the layer shifts $|u(x, z)|$ around the core; the symbol "−" labels the layers located at $z < 0$; "+" labels the layers from the upper half.

with the field of view Δz being only 50–90 nm, the variation $\Delta\varphi$ across Δz is less than 2°. In bounded samples, surface anchoring of the director can partially or completely suppress this rotation and favor selected values of φ. The states with $\varphi = \pi/2$ correspond to the tangential alignment of molecules at the substrates, while for $\varphi = 0$, there is a small surface tilt, comparable to $\theta_0 \sim 10°$.

The distinctive feature of the A dislocation is asymmetry of layers displacements above and below the plane $z = 0$, Figs. 2(c) and 4(a). The effect can be related to the elastic coupling between the layer deformations and the local tilt θ that is different from the equilibrium value θ_0 in a uniform sample. As shown in Fig. 4(a) in an approximation of a uniform director, the tilt $\partial u/\partial x$ of layers around the A dislocation imposes a larger molecular tilt $\theta > \theta_0$ for $z > 0$ and a smaller tilt $\theta < \theta_0$ for $z < 0$. The energy density of the distorted SmC^* with a fixed φ can be expressed through the layers deformations and the local θ, as $f_c = B[\partial u/\partial x - \frac{1}{2}(\partial u/\partial x)^2 + \frac{1}{2}\theta^2]^2/2 + K(\partial^2 u/\partial x^2)^2/2$ [21]. Here, B is the Young's modulus and K is the curvature

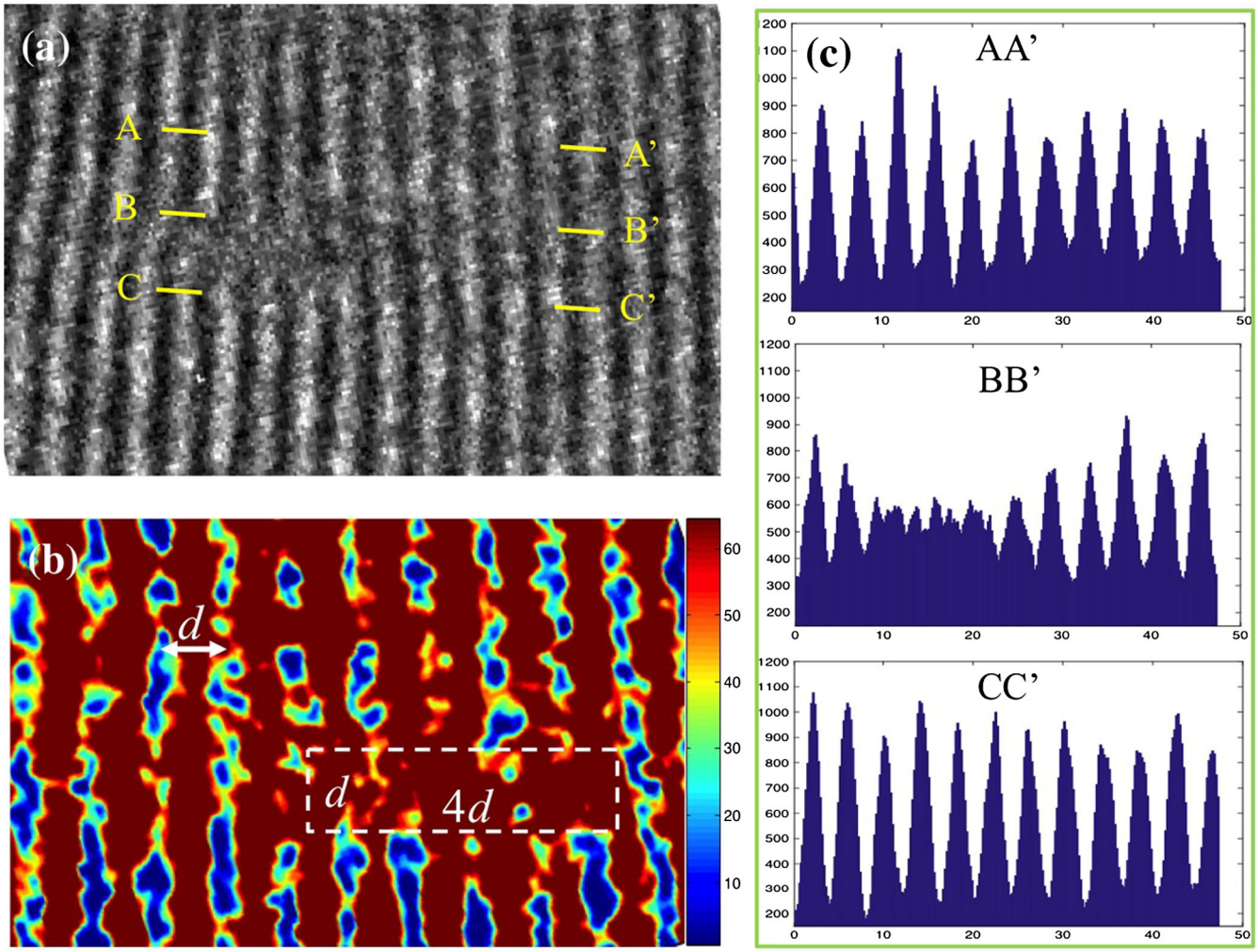

FIG. 3 (color online). Split-core S edge dislocations. (a) Gray-scale TEM image of an area with split-core edge dislocation. (b) A color-enhanced TEM image of another area with split-core edge dislocation. Dotted rectangle covers the split core with the aspect ratio 4:1. (c) Transmitted electron density profiles measured along the lines $\boldsymbol{AA}'$, $\boldsymbol{BB}'$, and $\boldsymbol{CC}'$ shown in part (a). Note the periodic nature of density variation along the lines $\boldsymbol{AA}'$ and $\boldsymbol{CC}'$ and reduction in the amplitude of modulations along the BB' line over a ~15 nm segment.

modulus. Since the energy density f_c should be about the same in the $z > 0$ and $z < 0$ semiplanes, different local tilt of molecules can produce different displacements, $u(x, z > 0) \neq u(x, z < 0)$, as indeed observed, Fig. 2(c). Interestingly, in the pioneering work on dislocations in wedge samples near the SmA-SmC phase transition, Meyer, Stebler, and Lagerwall [9] stressed that the optical features are consistent with $\varphi = \pi/2$; the asymmetry of displacements could not be verified since the dislocations were viewed along **b**.

In the nematiclike S core, the director is twisted to accommodate different thickness of the layers on both sides of the GP, Fig. 4(b). The anisotropic nature of the S core can be connected to the elastic properties of the medium by calculating the line tension of dislocation [12,22], neglecting nonlinear effects [19,23]. The layers displacements around the dislocation are described as $u(x, z) = -(b/4)\mathrm{sgn}(z)[1 + \mathrm{erf}(x/2\sqrt{\lambda z})]$, where $\lambda = \sqrt{K/B}$ [18]. The line tension F is then calculated by integrating the free energy density $f_c = \frac{1}{2}B(\partial u/\partial z)^2 + \frac{1}{2}K(\partial^2 u/\partial x^2)^2$ over the xz plane, excluding a rectangular core area $|x| \leq \xi_x, |z| \leq \xi_z$. The result [22], $F = (Kb^2/3\pi\xi_x\lambda) + F_c$, contains the core energy F_c that can be presented as $F_c = 2\xi_z\sigma_z$, where the energy density σ_z is associated with the director twist, from $\theta_0 + \delta/2$ to $\theta_0 - \delta/2$, as one crosses the core along the x axis, Fig. 4(b). The twist angle δ is determined by the number n of layers suffering a discontinuity. To estimate the relationship, we equate the total thickness $(n + 1)d'$ of the layers on one side of the core to the similar quantity nd'' on the other side; here $d' \approx l\cos(\theta_0 + \delta/2)$ and $d'' \approx l\cos(\theta_0 - \delta/2)$. Then $\delta \approx \cot\theta_0/n$. As a result, the core energy $F_c = 2K[(\cot\theta_0/2n\xi_x) - \hat{q}]^2\xi_x\xi_z \approx (1/2n)K\cot^2\theta_0$ decreases as n becomes larger; the latter explains the tendency of the core to split along the z axis. In the last expression, $\hat{q} \sim 0.3/\mu$m is neglected since it is much smaller than

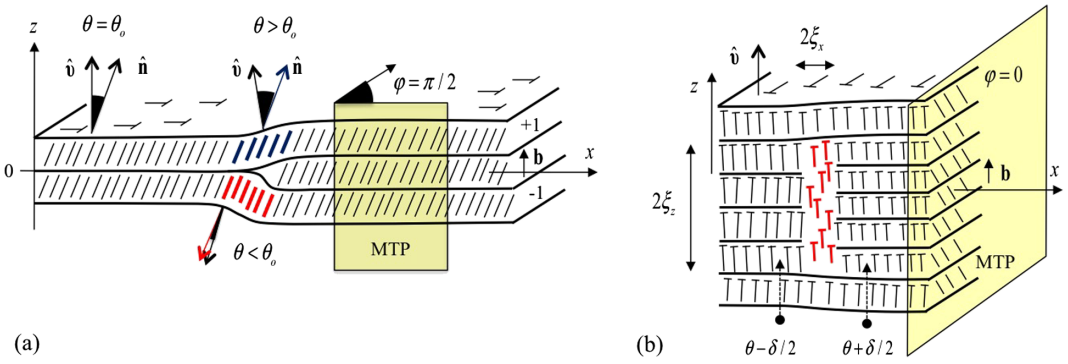

FIG. 4 (color online). Schematic images of A (a) and S (b) types of elementary edge dislocations in SmC^*. The nails show molecules tilted with respect to the plane of view; the heads are closer to the viewer than the ends. The layers tilt in (a) creates a different polar angle of the molecular tilt θ above and below the plane $z = 0$. Within the S core, the predominant director deformation is twist. Note the different direction of azimuthal tilt with respect to the glide plane of the dislocation, $\varphi = \pi/2$ in (a) and $\varphi = 0$ in (b).

$1/n\xi_x$. With $\xi_x = d/2$ and $\xi_z = nd/2$, one rewrites the line tension as $F = (16nK/3\pi) + (K\cot^2\theta_0/2n)$. Minimization with respect to n yields $n = \sqrt{(3\pi/32)}\cot\theta_0$. The estimate yields $n \approx 4$ for $\theta_0 \sim 10°$, which correlates well with the experiment.

To conclude, we presented the first experimental observations of the nanoscale details of elementary edge dislocations in a weakly twisted smectic C^*. We found two types of dislocations, an A type with an asymmetric profile of layers in the top and bottom semiplanes, and an S split type with the core strongly elongated along the Burgers vector and involving more than one melted smectic layer. We connect the observed features to the elastic coupling between the layer distortions and molecular polar and azimuthal tilts within the layers. In the A dislocations, the molecules tilt in the direction perpendicular to the dislocation's axis, while in the S dislocations, the molecular tilts are parallel to the defect's axis. The experimental observations pose a challenging problem of incorporating the polar and azimuthal components of the molecular tilts into the theoretical models of edge dislocations, especially at the core where the vanishing smectic order varies in space and couples to the orientational degrees of freedom; to the best of our knowledge, this problem has not been treated so far.

This work was supported by Grants No. DMR-1410378 and No. DMR-1307674. The TEM data were obtained at the cryo-TEM facility at the Liquid Crystal Institute, Kent State University, supported by the Ohio Research Scholars Program "Research Cluster on Surfaces in Advanced Materials" with the help of Dr. M. Gao. We thank R. Kamien for discussions and M. Salili for help with the data.

*olavrent@kent.edu

[1] M. Kleman and J. Friedel, Rev. Mod. Phys. **80**, 61 (2008).
[2] J. Friedel, *Dislocations* (Pergamon Press, New York, 1964).
[3] M. Kleman, O. D. Lavrentovich, and Y. A. Nastishin, in *Dislocations Solids*, edited by F. R. N. Nabarro and J. P. Hirth (ElsevierAmsterdam, Amsterdam, 2004), Vol. 12, p. 147.
[4] S. Fujii, S. Komura, and C.-Y. D. Lu, Soft Matter **10**, 5289 (2014).
[5] C. Blanc, N. Zuodar, I. Lelidis, M. Kleman, and J.-L. Martin, Phys. Rev. E **69**, 011705 (2004).
[6] M. Ambrožič, S. Kralj, T. J. Sluckin, S. Žumer, and D. Svenšek, Phys. Rev. E **70**, 051704 (2004).
[7] P. Oswald, J. Milette, S. Relaix, L. Reven, A. Dequidt, and L. Lejcek, Europhys. Lett. **103**, 46004 (2013).
[8] N. M. Abukhdeir and A. D. Rey, Soft Matter **6**, 1117 (2010).
[9] R. B. Meyer, B. Stebler, and S. T. Lagerwall, Phys. Rev. Lett. **41**, 1393 (1978).
[10] W. K. Chan and W. W. Webb, J. Phys. (Paris), Lett. **42**, 1007 (1981).
[11] A. M. Grubb, C. Zhang, A. Jákli, P. Sampson, and A. J. Seed, Liq. Cryst. **39**, 1175 (2012).
[12] M. Allain and M. Kleman, J. Phys. (Paris), Lett. **48**, 1799 (1987).
[13] C. Zhang, M. Gao, N. J. Diorio, W. Weissflog, U. Baumeister, S. N. Sprunt, J. T. Gleeson, and A. Jákli, Phys. Rev. Lett. **109**, 107802 (2012).
[14] C. Zhang, B. K. Sadashiva, O. D. Lavrentovich, and A. Jákli, Liq. Cryst. **40**, 1636 (2013).
[15] C. Zhang, N. Diorio, O. D. Lavrentovich, and A. Jákli, Nat. Commun. **5**, 3302 (2014).
[16] M. Gao, Y. Kim, C. Zhang, V. Borshch, S. Zhou, A. Jákli, O. D. Lavrentovich, M. Tamba, G. H. Mehl, D. Studer, B. Zuber, H. Gnägi, and F. Lin, Microsc. Res. Tech. **77**, 754 (2014).
[17] T. Ishikawa and O. D. Lavrentovich, Phys. Rev. E **60**, R5037 (1999).
[18] P. G. de Gennes, CR Hebd. Séances Acad. Sci. **275B**, 939 (1972).
[19] E. A. Brener and V. I. Marchenko, Phys. Rev. E **59**, R4752 (1999).
[20] C. Santangelo and R. D. Kamien, Phys. Rev. Lett. **91**, 045506 (2003).
[21] A. N. Shalaginov, L. D. Hazelwood, and T. J. Sluckin, Phys. Rev. E **60**, 4199 (1999).
[22] I. I. Smalyukh and O. D. Lavrentovich, Phys. Rev. E **66**, 051703 (2002).
[23] C. D. Santangelo and R. D. Kamien, Proc. R. Soc. A **461**, 2911 (2005).